Ab Initio Description of High-Temperature Superconductivity in Dense Molecular Hydrogen

P. Cudazzo,[1] G. Profeta,[1] A. Sanna,[2,3] A. Floris,[3] A. Continenza,[1] S. Massidda,[2] and E. K. U. Gross[3]

[1]*CNISM - Dipartimento di Fisica, Università degli Studi dell'Aquila, Via Vetoio 10, I-67010 Coppito (L'Aquila) Italy*
[2]*SLACS-INFM/CNR—Dipartimento di Fisica, Università degli Studi di Cagliari, I-09124 Monserrato (CA), Italy*
[3]*Institut für Theoretische Physik, Freie Universität Berlin, Arnimallee 14, D-14195 Berlin, Germany*

(Received 7 December 2007; published 23 June 2008; corrected 27 June 2008)

We present a first-principles study of the electron-phonon interaction and the prediction of the superconducting critical temperature in molecular metallic hydrogen. Our study is able to single out the features which drive the system towards superconductivity: mainly, a rich and complex Fermi surface and strongly coupled phonon modes driving the intra- or intermolecular charge transfer. We demonstrate that in this simple system, a very high superconducting critical temperature can be reached via electron-phonon and Coulomb electron-electron interactions.

DOI: 10.1103/PhysRevLett.100.257001 PACS numbers: 74.62.Fj, 74.20.−z, 74.25.Jb, 74.25.Kc

Hydrogen might seem the simplest element in the periodic table; however, it exhibits many puzzling and unusual properties which still remain undisclosed, despite the enormous efforts dedicated by quantum physicists. The results of this intense research effort made it clear that hydrogen is not simple at all: as an example, its (P, T) phase diagram is among the most complicated ones [1,2] and only very recently (partially) accessible to experiments [3,4].

The possibility of high-temperature superconductivity in metallic hydrogen, suggested in 1968 by N. W. Ashcroft [5], represents one of the most fascinating and intriguing topics and involves very fundamental issues ranging from the theoretical understanding of the limits of electron-phonon superconductivity, to implications in astrophysics [6]. In fact, based on the simple Bardeen-Cooper-Schrieffer (BCS) theory of superconductivity, we can understand why metallic hydrogen could be a good superconductor [5]: this system has very high phonon frequencies due to the light H mass, and it has a possibly strong electron-phonon interaction related to the lack of core electrons and to the quite strong covalent bonding. Many studies, aiming at investigating further this possibility [7,8], collected strong evidence pointing to high-T_c superconductivity; at the moment; however, the full scenario is still far from being clear and well established. One of the difficulties stems from the need of an adequate theoretical approach to the superconducting properties, relying on a full and consistent treatment of the electron-phonon (e-ph) and of the repulsive electron-electron (e-e) interaction [7,9].

In this Letter, we present a fully *ab initio* prediction of superconductivity in solid metallic hydrogen, based on the recently introduced density functional theory of superconducting state (SCDFT) [10,11]. This approach has been successful in the study of materials at ambient [12–14] and high [15] pressure. We show that molecular hydrogen gathers many peculiarities and fascinating features favoring the occurrence of the superconducting (SC) phase. We find an electron-phonon superconductivity in the *Cmca* structure (see later), with critical temperature (T_c) values up to 242 K at 450 GPa. Our calculations reveal a Fermi surface (FS) with many different and nonconnected sheets, strongly coupled with inter- and intramolecular phonon modes. This combination gives rise to anisotropic, multiband superconductivity.

Within SCDFT [10,11], we treat both e-ph and e-e interactions on the same ground, overcoming the difficulties related to the treatment of the Coulomb interaction, normally included, in the context of the Eliashberg theory, through the Morel-Anderson pseudopotential μ^* [16]. In fact, the need to include a more elaborate Coulomb interaction in the case of H under high pressure is in line with the conclusions of Richardson and Ashcroft [7]. Our predictions are based on normal state results obtained within a plane-wave [17] density functional theory approach, in the local density approximation (DFT-LDA). Phonons and e-ph interaction matrix elements are obtained within the density functional perturbation theory [18], while the screened e-e matrix elements are calculated in the static RPA approximation [19].

We first address the problem of the structural phases of metallic hydrogen. A *liquid* metallic phase at high pressure has been suggested based on the existence of a maximum in the melting curve of the (P, T) phase diagram [20]. In any case, proton quantum effects [21] would not allow, by now, a complete and accurate *ab initio* approach.

On the other hand, solid phases are accessible to first-principles methods, as confirmed by earlier DFT-LDA calculations of the $T = 0$ K phase diagram [1]. In addition, the competition among possible candidate phases has been recently addressed through an extended first-principles study by Pickard and Needs [2] who pointed to the metallic *Cmca* phase as the most stable in a pressure interval between $\simeq$ 400 and 500 GPa.

The stability of the metallic *Cmca* phase (above 150 GPa) has been previously anticipated by Johnson and Ashcroft [1]; however, the well-known band-gap problem within density functional theory severely hindered the

determination of a reliable pressure value where metallization would set in. Recently, exact-exchange calculations [22] fixed the metallization pressure of the *Cmca* phase at $\simeq 400$ GPa, consistently with experimental evidence [3] showing no signs of metallicity up to about 320 GPa. Being focused on SC properties, we thus consider the *Cmca* solid hydrogen phase in the range between 400 and 500 GPa, well within the limits set by the metallization and the phase transition to the monatomic metallic phase [1].

The *Cmca*-phase has a base-centered orthorhombic (bco) unit cell with one molecule in the $z = 0$ plane and one in the $z = c/2$ plane [1], having opposite orientations (see inset of Fig. 1). Starting from the simple picture of bonding and antibonding H_2 molecular orbital, valid at $P = 0$, the evolution of the electronic structure with pressure can be described on the basis of intermolecular bonding and antibonding combinations between the two H_2 molecules in the unit cell. The corresponding four energy bands will be referred to as $\varepsilon_{ij,\mathbf{k}}$ ($i, j = b, a$ define bonding and antibonding combinations; the first and second indices refer to intra and intermolecular character, respectively).

The bonding (antibonding) combination of the molecular H_2 bonding states are always completely (almost completely) occupied in all the pressure ranges (up to 500 GPa), preserving the stability of the H_2 molecule (see Fig. 1). However, at the metallization pressure, the progressive overlap between $\varepsilon_{ba,\mathbf{k}}$ and $\varepsilon_{ab,\mathbf{k}}$ sets a competition between intra and intermolecular bonding, eventually leading to a monatomic metallic phase. In fact, $\varepsilon_{ba,\mathbf{k}}$ rises above the Fermi level (E_F) while the higher energy bands, and in particular $\varepsilon_{ab,\mathbf{k}}$, drop below E_F in some regions of the Brillouin zone (BZ). This results in a charge transfer from intramolecular toward intermolecular bonds and in the formation of several electron and hole pockets at E_F. The Fermi surface becomes particularly rich and complex (Fig. 2) and provides the strong *e*-ph coupling necessary to superconductivity (see below).

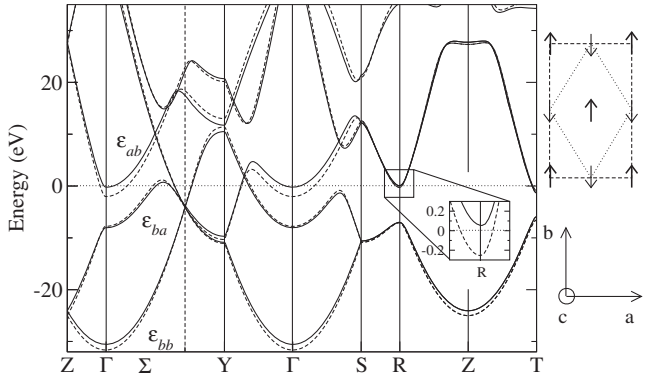

FIG. 1. Electronic band structure of the *Cmca*-phase at 414 (solid line) and 462 (dashed line) GPa and schematic view of the *Cmca*-phase, with the orthorhombic (dashed line) and bco (dotted line) unit cell. Bold (thin) arrows represent molecules at the $z = 0$ ($z = c/2$) plane.

Three types of bands form the Fermi surface at high pressure: the two tubular structures intersecting the k_y axis and the two "prismlike" structures along the k_x axis originate from $\varepsilon_{ba,\mathbf{k}}$and have hole-type character; the disk centered at the Γ-point ($\varepsilon_{ab,\mathbf{k}}$) and the structures near the *C*-point ($\varepsilon_{aa,\mathbf{k}}$) have electron-type character; the remaining sheets are related to degenerate $\varepsilon_{ab,\mathbf{k}}$ and $\varepsilon_{aa,\mathbf{k}}$ orbitals along $Z - T$. The different orbital character of the FS branches suggests the occurrence of different couplings between the various bands, leading to an anisotropic SC gap and, possibly, to a multigap superconductivity. This last feature is particularly interesting, as it is not so common and may favor a significant T_c enhancement [12,23,24].

The molecular nature of the charge density distribution gives rise to an intriguing phonon dispersion (Fig. 3). The phonon modes can be grouped into three main branches: *phononic*, *libronic*, and *vibronic*, corresponding, respectively, to the relative translations, rotations, and internal vibrations of the H_2 molecules. We immediately notice the presence of several anomalies: in particular, we see the high frequencies vibronic modes dropping from 4000 cm^{-1} at the BZ boundary to 3000 cm^{-1} close to the $\mathbf{q} = \Gamma$ point and the lower frequency libronic modes dropping from $\simeq 2000$ to 1000 cm^{-1}. The softening of the modes is related to a strongly $\mathbf{q}$-dependent *e*-ph contribution to the phonon self-energy. In fact, we find a strong intraband ($\mathbf{q} = 0$) coupling between the FS features close to the $\mathbf{k} = \Gamma$ point ($\varepsilon_{ab,\mathbf{k}}$ states) and the out-of-phase libronic mode; a strong coupling also occurs between the

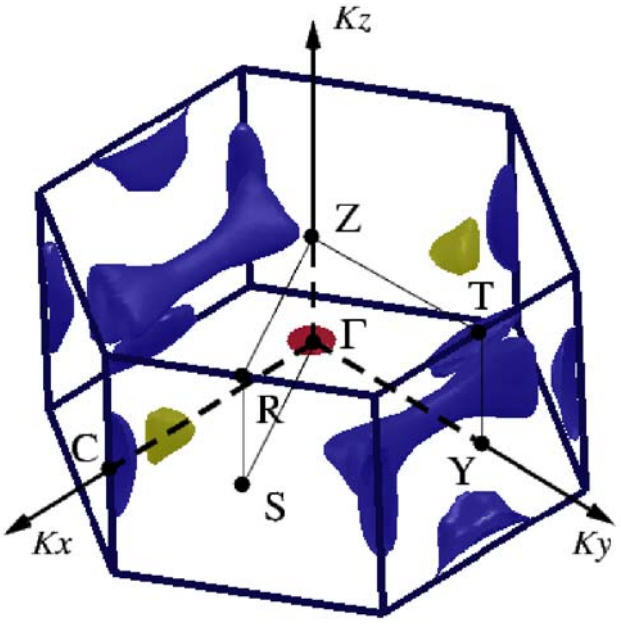

FIG. 2 (color online). Fermi surface and gap values at 414 GPa showing the disk at the Γ-point ($18.0 < \Delta < 21$ meV), the "prismlike" structures ($13.6 < \Delta < 18.0$ meV), and the other sheets ($10.0 < \Delta < 13.6$ meV).

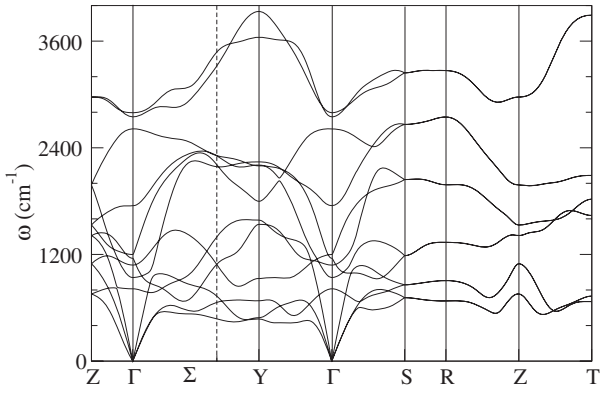

FIG. 3. Phonon dispersion at 414 GPa.

two "prismlike" Fermi sheets ($\varepsilon_{ba,\mathbf{k}}$) and the softened vibronic modes, able to activate charge transfer within intra- and intermolecular states. While strongly renormalized zone-center phonons contribute to the coupling within individual FS sheets, high-$\mathbf{q}$ scattering, mainly coming from *phononic* modes, gives rise to interband transitions between the various FS's, coupling bonding states within the H-layer to interlayer states. The presence of multiple Fermi surfaces provides a "$\mathbf{q}$-distributed" coupling, with several modes contributing to the pairing; this allows to increase λ still avoiding a lattice instability, which could result from very high coupling at some specific $\mathbf{q}$'s. In fact, the Eliashberg function (Fig. 4) shows three main frequency regions, *all* of them strongly coupled to the electrons and associated with phononic, libronic, and vibronic modes, in an increasing frequency order; however, a net distinction between phononic and libronic modes is prevented due to the branch mixing caused by the large renormalization of the libronic modes. As the pressure rises, the coupling increases, and a new feature appears at ≈ 1700 cm^{-1}. The first effect is due to the increasing density of states at E_F and to interband (high-$\mathbf{q}$) scattering with *phononic* modes and intraband scattering with softened libronic modes at $\mathbf{q} = \Gamma$: as the molecular distance along the c axis shortens, the interlayer charge keeps growing and becomes very sensitive to molecular rotation and translation. The additional peak in the $\alpha^2F(\omega)$ comes from an extra band ($\varepsilon_{ab,\mathbf{k}}$) which crosses the Fermi level close to R point (see inset in Fig. 1). This creates a new electron-type Fermi sheet, strongly coupled with in phase libronic modes, and opens a further coupling channel at higher pressure giving rise to a jump in λ at ≈ 435 GPa.

Note that the e-ph coupling is not monotonic with pressure: the increased metallization progressively brings the system towards a more free-electronlike state, where the electron-ion interaction is more efficiently screened out. Although rather large, the values of λ are of the same order as, e.g., those obtained in fcc-Li under high pressure (40 GPa), leading to $T_c \simeq 20$ K. In the case of hydrogen, we expect that the large phonon frequencies provided by the H_2 vibronic modes may lead to much higher T_c's.

The T_c was calculated solving the SCDFT anisotropic gap equation. The e-ph matrix elements as well as the RPA screened Coulomb repulsion were treated on equal footing and without any averaging process, i.e., with full $\mathbf{k}$-dependence. As previously shown in the case of low-density metals [15], and discussed by Richardson and Ashcroft [9], a complete inclusion of both interactions is crucial to reproduce experimental T_c's. We find very high T_c's, considerably increasing with pressure up to 242 K at 450 GPa (see Fig. 5). Comparing the insets of Figs. 4 and 5, it is clear that T_c follows closely the λ behavior with pressure. As anticipated, we predict a multigap (three-gap) superconductivity, which is progressively lost at

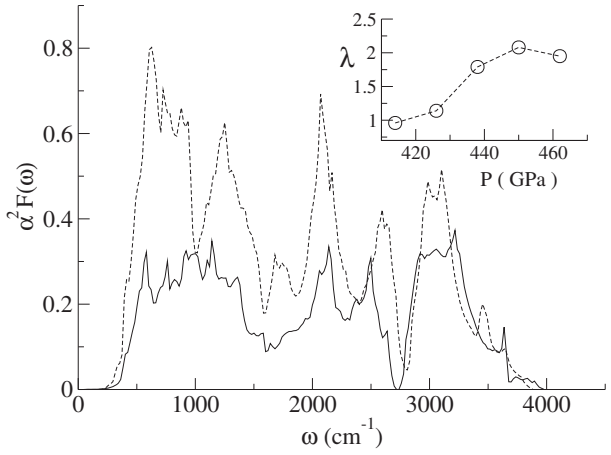

FIG. 4. $\alpha^2F(\Omega)$ at 414 (solid line) and 462 (dashed line) GPa. The inset shows the electron-phonon coupling (λ) as a function of pressure.

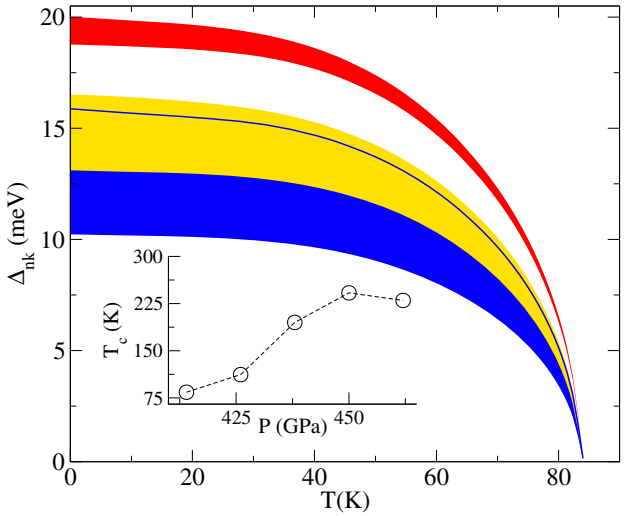

FIG. 5 (color online). $\Delta_{n\mathbf{k}}$ at E_F at 414 GPa. The shaded regions represent the $\mathbf{k}$-anisotropy over different bands (note the overlap from 13.00 to 15.75 meV). The inset shows the superconducting critical temperature as a function of pressure.

high pressure, where interband scattering raises the nondiagonal $\lambda_{nn'}$ matrix elements, leading to a merging of the different gaps.

The occurrence of multigap superconductivity is clearly illustrated in Fig. 5, which plots the gap $\Delta_{n\mathbf{k}}$ at the Fermi level as a function of temperature [for all the bands (n) and $\mathbf{k}$-points] at the pressure with larger band anisotropy, $P = 414$ GPa ($T_c = 84$ K). The three gaps are evident: the largest one at $\simeq 19.3$ meV, and two very anisotropic, overlapping gaps at 15.4 and 13.6 meV. The three gaps are associated with different FS sheets (cf. Fig. 2): the strongly coupled disk around the Γ-point, the ''prismlike'' sheets, and the others associated with the lowest gap.

Our completely *ab initio* approach gives us confidence to draw reliable conclusions on the superconducting phase of molecular metallic H. However, there are relevant issues concerning this peculiar system that must be addressed: (i) an explicit treatment of the electron screening is required. In fact, the use of a single value for the parameter μ^*, as an ''effective'' Coulomb pseudopotential is formally unjustified [7], due to the different character of the orbitals and the multigap nature. The calculation of the Coulomb matrix elements confirms that the repulsion depends on the orbital nature of the Fermi surface. In addition, the average unrenormalized repulsive Coulomb interaction (μ) increases from 0.22 at 414 GPa to 0.28 at 462 GPa. (ii) In our calculations, we considered the screened electron-electron interaction within the RPA approximation for the dielectric constant. However, perturbation theory in the electron-electron interaction beyond RPA can produce an additional effective attractive interaction in a multiband system as hydrogen [9,25]. This additional pairing channel can only increase the critical temperature [26]. (iii) At the insulator-metal transition, the electron and hole pockets at FS have rather small Fermi energy (0.2–0.3 eV). Because of the very large phonon frequencies involved, nonadiabatic effects and vertex corrections beyond the Migdal approximation can be expected [27]; however, inclusion of such contributions into an *ab initio* theory is not easy at all, and the effect on T_c is presently far from being obvious.

In conclusion, state of the art *ab initio* calculations of superconducting properties have been presented for molecular hydrogen under high pressure. Apart from the astonishingly high critical temperatures predicted, the analysis of the electronic and dynamical properties of the studied system points to the origin of superconductivity. In particular: (i) we confirm a strong electron-phonon coupling, increasing with pressure; (ii) the presence of multiple Fermi surfaces with different character provides both strong intraband (low-$\mathbf{q}$) and interband (high-$\mathbf{q}$) electron-phonon scattering. In this respect, (iii) a major role is played by the molecular rotational (libronic) and vibrational (vibronic) modes, which are strongly coupled with the intermolecular charge. Finally, (iv) we predict three superconducting gaps at the Fermi level, associated with Fermi surface branches having different character. We hope that this study will stimulate the search for new molecular and metallic systems sharing these same favorable features.

The authors acknowledge S. Scandolo for suggesting the topic and S. Scandolo and L. Burderi for valuable discussions. Work partially supported by the Italian Ministry of Education, through PRIN 200602174 project and through PON-CyberSar (Consorzio COSMOLAB), by INFM-CNR through a supercomputing grant at Cineca (Bologna, Italy), by the Deutsche Forschungsgemeinschaft and by NANOQUANTA Network of Excellence.

[1] K. A. Johnson and N. W. Ashcroft, Nature (London) **403**, 632 (2000).
[2] C. J. Pickard and R. J. Needs, Nature Phys. **3**, 473 (2007).
[3] P. Loubeyre *et al.*, Nature (London) **416**, 613 (2002).
[4] I. Goncharenko and P. Loubeyre, Nature (London) **435**, 1206 (2005).
[5] N. W. Ashcroft, Phys. Rev. Lett. **21**, 1748 (1968).
[6] N. W. Ashcroft, J. Phys. Condens. Matter **16**, S945 (2004).
[7] C. F. Richardson and N. W. Ashcroft, Phys. Rev. Lett. **78**, 118 (1997).
[8] N. Barbee III *et al.*, Nature (London) **340**, 369 (1989).
[9] C. F. Richardson and N. W. Ashcroft, Phys. Rev. B **55**, 15130 (1997).
[10] M. Lüders *et al.*, Phys. Rev. B **72**, 024545 (2005).
[11] M. A. L. Marques *et al.*, Phys. Rev. B **72**, 024546 (2005).
[12] A. Floris *et al.*, Phys. Rev. Lett. **94**, 037004 (2005).
[13] A. Sanna *et al.*, Phys. Rev. B **75**, 020511(R) (2007).
[14] A. Floris *et al.*, Phys. Rev. B **75**, 054508 (2007).
[15] G. Profeta *et al.*, Phys. Rev. Lett. **96**, 047003 (2006).
[16] P. Morel and P. W. Anderson, Phys. Rev. **125**, 1263 (1962).
[17] S. Baroni *et al.*, http://www.quantum-espresso.org. Computational details: We used a norm conserving pseudopotential with energy cutoff of 60 Ry. 12^3 k-points mesh for self-consistence and 26^3 for phonon calculation on a 6^3 q-points grid. Kernels were evaluated at 16^3 k-points and 6^3 q-points; the SCDFT gap equation was solved with 6×10^3 k-points close to the FS.
[18] S. Baroni *et al.*, Rev. Mod. Phys. **73**, 515 (2001).
[19] A. Marini *et al.*, SELF code, (http://www.fisica.uniroma2.it/~self/).
[20] S. A. Bonev *et al.*, Nature (London) **431**, 669 (2004).
[21] E. Babaev *et al.*, Nature (London) **431**, 666 (2004).
[22] M. Städele and R. M. Martin, Phys. Rev. Lett. **84**, 6070 (2000).
[23] A. Y. Liu *et al.*, Phys. Rev. Lett. **87**, 087005 (2001).
[24] H. J. Choi *et al.*, Phys. Rev. B **66**, 020513 (2002).
[25] G. Vignale and K. S. Singwi, Phys. Rev. B **31**, 2729 (1985).
[26] The corrections could be easily cast into the SCDFT method and will be the subject of future work.
[27] E. Cappelluti *et al.*, Phys. Rev. Lett. **88**, 117003 (2002).